

Continental erosion and the Cenozoic rise of marine diatoms

Pedro Cermeño^{a,1}, Paul G. Falkowski^{b,c}, Oscar E. Romero^d, Morgana F. Schaller^e, and Sergio M. Vallina^a

^aDepartamento de Biología Marina y Oceanografía, Instituto de Ciencias del Mar, 08003 Barcelona, Spain; ^bEnvironmental Biophysics and Molecular Ecology Program, Department of Marine and Coastal Sciences, Rutgers University, New Brunswick, NJ 08901; ^cDepartment of Earth and Planetary Sciences, Rutgers University, Piscataway, NJ 08854; ^dMARUM - Center for Marine Environmental Sciences, University of Bremen, 28359 Bremen, Germany; and ^eEarth and Environmental Science, Rensselaer Polytechnic Institute, Troy, NY 12180

Edited by Donald E. Canfield, Institute of Biology and Nordic Center for Earth Evolution, University of Southern Denmark, Odense M, Denmark, and approved February 23, 2015 (received for review July 8, 2014)

Marine diatoms are silica-precipitating microalgae that account for over half of organic carbon burial in marine sediments and thus they play a key role in the global carbon cycle. Their evolutionary expansion during the Cenozoic era (66 Ma to present) has been associated with a superior competitive ability for silicic acid relative to other siliceous plankton such as radiolarians, which evolved by reducing the weight of their silica test. Here we use a mathematical model in which diatoms and radiolarians compete for silicic acid to show that the observed reduction in the weight of radiolarian tests is insufficient to explain the rise of diatoms. Using the lithium isotope record of seawater as a proxy of silicate rock weathering and erosion, we calculate changes in the input flux of silicic acid to the oceans. Our results indicate that the long-term massive erosion of continental silicates was critical to the subsequent success of diatoms in marine ecosystems over the last 40 My and suggest an increase in the strength and efficiency of the oceanic biological pump over this period.

marine diatoms | continental erosion | silicic acid | biological pump | Cenozoic era

Unlike the majority of other phytoplankton, diatoms (unicellular photosynthetic microalgae) depend on the availability of silicic acid (in the form of orthosilicic acid— H_4SiO_4) to construct their cell walls (1, 2). Once the supply of H_4SiO_4 is exhausted, diatom blooms collapse and a large fraction sinks rapidly out of the surface layer to the ocean interior (Fig. 1). Over geological time, this phenomenon is thought to have decreased the concentration of H_4SiO_4 in the surface waters of the oceans to unprecedented levels in the history of Earth systems (3, 4), with important consequences for the biogeographic distribution and morphometric evolution of marine silicifiers (5–7).

Like diatoms, radiolarians (amoeboid protozoa, some of which harbor photosynthetic symbiotic algae) build intricate tests of amorphous silica by precipitating H_4SiO_4 from seawater. Fossil evidence strongly suggests that the rise of marine diatom diversity over the latter half of the Cenozoic era is mirrored by a simultaneous decrease in the weight of radiolarian tests (7–9), suggesting that an increasingly larger proportion of the ocean silica reservoir has been appropriated by diatoms. The most pronounced decrease in radiolarian test weight is coeval with a pulse of diatom diversity across the Eocene–Oligocene (E/O) transition (~38–32 Ma), supporting the hypothesis that competition for H_4SiO_4 played a role in the rise of diatoms (7, 8). This evolutionary model assumes a constant (steady-state) input of H_4SiO_4 to the ocean. However, changes in the rates of continental weathering and erosion could also increase the concentration of H_4SiO_4 in the surface waters of the oceans over geological time, and thus represent a plausible alternative hypothesis for the rise of diatoms to ecological prominence (10, 11). Here we combine the analysis of data from sedimentary records with numerical simulations to quantify the extent to which the erosion of continental silicates facilitated the ecological expansion of marine diatoms during the Cenozoic era.

Results and Discussion

The Summed Common species Occurrence Rate (SCOR) quantifies changes in the extent to which species were common and geographically widespread from the fossil record (12). This index is based on the assumption that the more globally abundant a species is, the more likely it is to occur in a greater number of sampling sites. Together with SCOR, the temporal dynamics of diversity generated from global deep sea sediment data compilations permit delineation of the evolutionary trajectories of marine planktonic diatoms over the period of study.

Marine diatoms exhibit two major pulses of diversification and geographic expansion during the Cenozoic (13–15) (Fig. 2A). The first pulse began in the late Eocene and attained a maximum in the early Oligocene (~38–31 Ma). The number of species and SCOR increased again in a second pulse that developed through the Miocene epoch (23–5.3 Ma) and extends until the present. This pattern is not observable for radiolarians, which exhibit more restricted geographic distributions and lower diversity through time (Fig. S1). Their fossil record indicates a secular trend of decreasing test weight throughout the Cenozoic (7, 8) (Fig. S2). This trend cannot readily be explained as a taphonomic artifact; if anything, it is opposite to a trend of poorer preservation in older fossils. Using three regression models (ordinary least squares, reduced major axis, and quadratic), and the first and last observation of each time series, we estimate an increase in diatom diversity and SCOR in the range 1.6- to 2.8-fold across the E/O transition, and between 1.9- and 3.1-fold from the early Miocene (~20 Ma) to present time (Fig. 3 and Table S1).

Significance

Diatoms are silica-precipitating microalgae responsible for roughly one-fifth of global primary production. The mechanisms that led these microorganisms to become one of the most prominent primary producers on Earth remain unclear. We explore the linkage between the erosion of continental silicates and the ecological success of marine diatoms over the last 40 My. We show that the diversification and geographic expansion of diatoms coincide with periods of increased continental weathering fluxes and silicic acid input to the oceans. On geological time scales, the ocean's biologically driven sequestration of organic carbon (the biological pump) is proportional to the input flux of inorganic nutrients to the oceans. Our results suggest that the strength and efficiency of the biological pump increased over geological time.

Author contributions: P.C. designed research; S.M.V. performed computational work; P.C., P.G.F., O.E.R., M.F.S., and S.M.V. analyzed data; and P.C., P.G.F., O.E.R., M.F.S., and S.M.V. wrote the paper.

The authors declare no conflict of interest.

This article is a PNAS Direct Submission.

¹To whom correspondence should be addressed. Email: pedrocermeno@icm.csic.es.

This article contains supporting information online at www.pnas.org/lookup/suppl/doi:10.1073/pnas.1412883112/-DCSupplemental.

Silicic acid [micromol/kg] @ Depth [m]=50

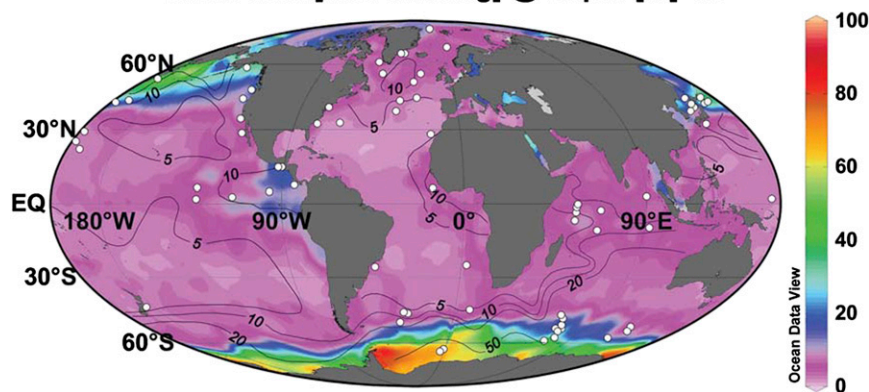


Fig. 1. Global map showing the surface concentration of silicic acid in the modern oceans. Although biogenic silica tends to dissolve throughout the water column and in the sediments, enough silica is buried to keep the surface ocean undersaturated (contour lines, % biogenic silica in sediments) (23). In the modern oceans, diatoms thrive along continental margins, the Equatorial Pacific, and the Southern Ocean where increased inputs of H_4SiO_4 stimulate their growth. The locations of the Deep Sea Drilling Project and Ocean Drilling Program sites used to delineate the evolutionary trajectory of diatoms are also plotted (dots).

The evolutionary histories of marine diatoms and radiolarians can be examined by using a chemostat-like model with two organisms competing in steady state for a single limiting nutrient. In this scenario, the growth demands for H_4SiO_4 of increasingly successful diatoms should be equivalent to a concomitant decrease in H_4SiO_4 use by radiolarians, which decreased their silica quota by decreasing the weight of their tests. We examined this hypothesis using a mathematical simulation model in which diatoms and radiolarians compete for H_4SiO_4 in a constant supply scenario. In the model, the silica to carbon (Si:C) ratio of radiolarians decreases through time, simulating a reduction in test weight. Simultaneously, an increasingly larger amount of H_4SiO_4 is allocated to diatoms, owing to their superior competitive ability. The model shows a modest <1.4-fold increase in diatom carbon biomass during the E/O transition regardless of the initial Si:C ratio of radiolarians (Fig. 3A, test weight). Similarly, the model predicts a <1.3-fold increase in diatom biomass from the early Miocene to the present (Fig. 3B, test weight). Thus, to the extent that the patterns of diversity and SCOR reported from fossil data are comparable to modeled changes in diatom biomass, our results suggest that this ecological strategy is insufficient to explain the ecological success of marine diatoms in any of the geological times investigated (Student's t test, $P < 0.01$).

Increased weathering of continental silicates is the most likely mechanism to account for additional inputs of H_4SiO_4 to the Cenozoic oceans. To explore this possibility, we analyzed the published lithium isotope record of seawater ($\delta^7\text{Li}$) (16), a proxy of silicate rock weathering style. Lithium is supplied to the oceans through volcanic activity and from the erosion of silicate rocks, while it is removed primarily by structural incorporation of dissolved lithium into marine sediments (reverse weathering). Lithium is present in the environment in two isotopic forms, ^7Li and ^6Li . The preferential uptake of ^6Li into secondary clay minerals formed during weathering leads to a large removal-induced fractionation (increasing seawater $\delta^7\text{Li}$) (17), which is recorded in the calcium carbonate shells of planktonic foraminifera. The record of seawater $\delta^7\text{Li}$ over the last 50 My is dominated by two punctuated rises that reflect enhanced rates of continental weathering and erosion, and a greater fraction of weathered minerals in the suspended fraction, which is largely attributed to the uplift of the Himalayas (16, 18). These increases in seawater $\delta^7\text{Li}$ (16) and geochemical evidence of increasing riverine weathering fluxes over the last 40 My (19) imply increased

inputs of silicates to the surface waters of the oceans, paralleling the rises of marine diatom diversity and SCOR across the E/O transition and through the Miocene.

Based on the lithium isotope record of weathering style (a transition from transport-limited to weathering-limited regimes) (16), and assuming a twofold increase in dissolved silica content in fluvial output over the last 50 My (20), we estimate a 20% increase in dissolved silica flux to the oceans across the E/O transition and an 80% increase through the Miocene (Fig. 2B) (see *Materials and Methods*). An increase of this order in the flux of H_4SiO_4 to the model system facilitated a 1.8-fold (± 0.2) increase in diatom biomass across the E/O transition (Fig. 3A, weathering) and 2.2-fold (± 0.2) during the Miocene (Fig. 3B, weathering). The increase in diatom biomass predicted by the model is of a magnitude similar to the increase in diatom diversity and SCOR estimated from fossil data (Fig. 3). A model sensitivity analysis provides a number of potential scenarios that strongly support the hypothesis that increased continental silicate weathering fluxes facilitated the rise of diatoms to ecological prominence (Fig. 4).

The patterns of diatom diversity and SCOR, and the associated changes in silicate weathering fluxes reported here, are consistent with the record of opal (biogenic silica) accumulation in sediments from the eastern equatorial Pacific, one of the largest of the siliceous depocenters throughout the Cenozoic, where Neogene opal accumulation rates are distinctly higher than those reported for the Eocene (21). Increased opal accumulation rates are also documented across the late Eocene and early Oligocene (22), synchronous with an inflection in the strontium and lithium isotope records and a shift in the mineral composition of clay assemblages in sediments from the Southern Ocean (16, 22), all indicative of increased weathering fluxes. Although silica input/output fluxes might be imbalanced on time scales shorter than the residence time of H_4SiO_4 in the ocean (tens of thousands of years) (23), our analysis of changing silicate weathering fluxes and their effect on diatom diversification encompasses time scales of million years. On these time scales, the ocean system can be treated as steady state with respect to silica, and therefore, unless the ancient silica cycle operated in a different mode, all of the H_4SiO_4 inputs from rock weathering should be equally removed by equivalent burial of biogenic silica in marine sediments.

Diatom diversity and SCOR from the early Oligocene to the early Miocene exhibit a conspicuous decrease. The observation that this pattern is also noticeable for radiolarians in the fossil

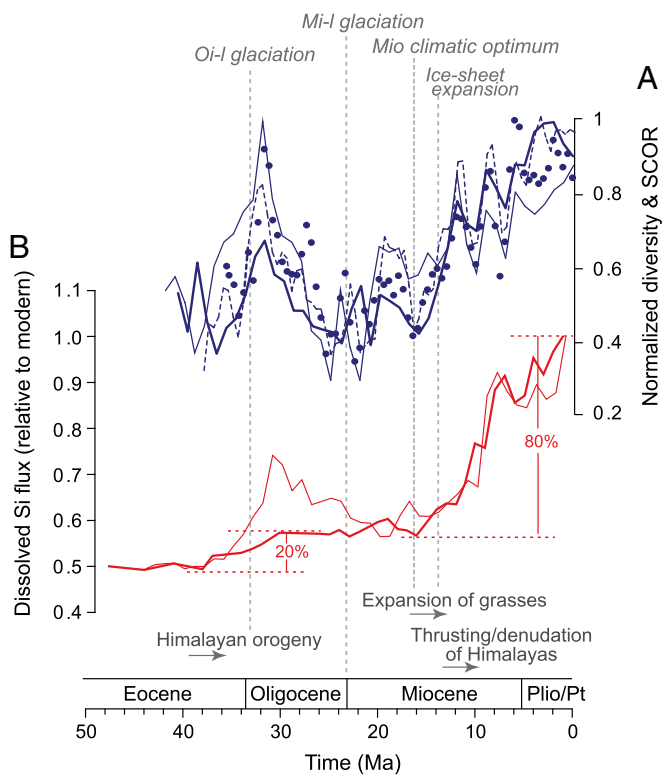


Fig. 2. Sedimentary records of marine planktonic diatoms and silica flux to the oceans based on global ocean data compilations. (A) Normalized diversity and SCOR. Diversity curves are generated using two different methods of sampling standardization, the unweighted lists subsampling method (UW, solid thin line) and the Shareholder Quorum Subsampling method (SQS, dashed thin line). Also represented is the consensus diversity curve (LBR, solid thick line) reported by Lazarus et al. (13) and SCOR (dots). (B) Fluxes of H_4SiO_4 to the global ocean based on the lithium isotope record (red thick line) and to the Southern Ocean based on marine sedimentary clays (red thin line) are both relative to modern fluxes.

record suggests that the cycling of silica could be a common cause. We associate this pattern with a long-term stabilization/reduction of weathering fluxes, which is in part recognized from the lithium isotope record (16) and a reverse shift in the mineral composition of marine sedimentary clays (Fig. S4). However, the transition into a four-layer vertical ocean configuration during the Oligocene (24) could also play a role. The circulation of intermediate waters in the contemporary ocean is strongly influenced by the Antarctic Circumpolar Current, which blocks warm surface waters from reaching Antarctica. In their route northward, intermediate waters feed low-latitude ecosystems, yet, in this ocean configuration, the Southern Ocean acts as a trap for H_4SiO_4 (25). The Antarctic Bottom Water (AABW) circulation cell is closed by AABW mixing into North Atlantic Depth Water (NADW). The dissolution of sinking opal from plankton occurs largely within the NADW and AABW, which bring H_4SiO_4 back to the surface in the vicinity of Antarctica, thereby limiting its spread elsewhere (25). In the warmer Oligocene ocean, the formation of deep waters in the North Pacific should have been as strong as in the North Atlantic and consequently may have mixed similarly with southern-sourced waters. This transition into a new ocean vertical structure led to a major reorganization of the oceanic inventory of H_4SiO_4 , perhaps exacerbating the crisis of siliceous plankton during the Oligocene, at least to the north of the sub-Antarctic front.

Our calculations of dissolved silica flux to the oceans assume that the global average ratio of suspended (clay) versus dissolved

silica in rivers increased from 1:4 to 4:1 over the Cenozoic in concert with changes in the suspended to dissolved lithium ratio (16). Recent compilations suggest that, at present, the suspended to dissolved silica ratio might be an order of magnitude larger (26, 27). An increase in this ratio would further substantiate our interpretation that the flux of H_4SiO_4 to the oceans increased greatly through the Miocene. However, these calculations suggest a relatively modest increase in the flux of H_4SiO_4 across the E/O transition. We speculate that the lithium isotope record, which is a global-scale integration of weathering styles (the residence time of lithium in seawater is ~ 1.2 My), may be insensitive to increased weathering fluxes to specific regions. The mineral composition of clays in marine sediments is also indicative of weathering style and provides a geographically localized estimate of continental erosion. Illite and chlorite tend to dominate clay assemblages in marine sediments near regions characterized by weathering-limited regimes where high erosion rates leave fresh rock surfaces continuously exposed to chemical weathering (28). Thus, dominance of illite and chlorite in marine sediments is indicative of increased continental weathering fluxes to the oceans. A compilation of clay data from Southern Ocean sediments shows an increase in the percentage of illite and chlorite across the E/O transition and through the Miocene consistent with the lithium isotope record of seawater (Fig. 2B and Fig. S4). The increase in the percentage of illite and chlorite across the E/O transition is remarkable and potentially associated with the expansion of Antarctic ice sheets and its effect on continental erosion.

Our analysis further assumes that, on geological time scales, the flux of dissolved silica to the oceans increased proportional to the flux of suspended silica in fluvial output. A recent compilation of data shows a positive relationship between suspended

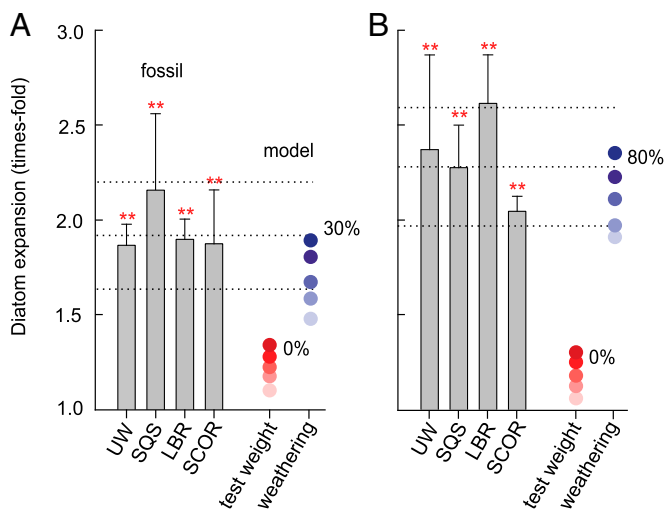


Fig. 3. Time fold increase in diatom diversity (UW, SQS, and LBR) and SCOR across the E/O transition (A), and from the early Miocene to present time (B) (bars). Error bars are the SD of the estimates generated from different analytical methods applied to calculate time fold increase (see SI Text, Table S1, and Fig. S3). The expansion of diatoms from model simulations is expressed as time fold increase in diatom carbon biomass (millimoles carbon per cubic meter) over the time interval of interest under two different scenarios, (i) a constant supply of H_4SiO_4 through time (test weight, red circles) and (ii) an increasing supply of H_4SiO_4 through time (weathering, blue circles). The sequence of colors denotes the initial Si:C ratio of radiolarians used in the simulations from 0.15 (lighter) to 1 (darker). Gray dashed lines are the mean and SD of the ensemble of estimates generated from fossil data. The percentages represent the increase in diatom biomass attributed to increased weathering fluxes. Asterisks above bars denote statistically significant differences among fossil data and model simulations under the constant H_4SiO_4 supply scenario (test weight).

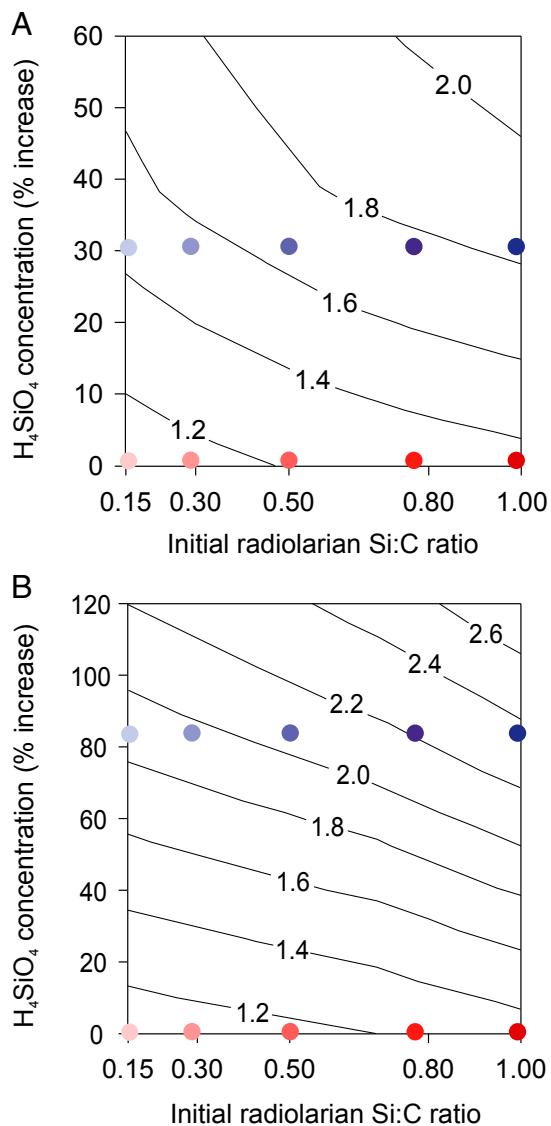


Fig. 4. Model sensitivity to changes in the concentration of H_4SiO_4 in the model system. Time fold increase in diatom biomass (contour lines) across the E/O transition (A) and the Miocene to present time period (B). We simulated a decrease in the weight of radiolarian tests through time by decreasing the initial Si:C ratio by 50% during the E/O transition and 30% during the Miocene according to an exponential decay function. Zero percent change in H_4SiO_4 concentration represents the scenario in which any increase in diatom biomass is associated exclusively with a decrease in the Si:C ratio of radiolarians. Colored circles denote model setups used to compose Fig. 3.

and dissolved silica yields (flux per unit surface area) to coastal regions of the world oceans (26). In support of this positive relationship, chemical weathering rates have been observed to increase with physical erosion in numerous geological settings (29, 30). The physical removal of soils continuously refreshes mineral surfaces and increases the rate of chemical weathering. Ultimately, continental weathering fluxes depend on runoff, lithology (29), topographic relief (18, 31), and geographic location with respect to large-scale persistent climate belts (32, 33) that are a function of Hadley circulation. To the extent that this relationship between physical erosion and chemical weathering extends over geological time, the lithium isotope record suggests substantial increase in H_4SiO_4 flux to the oceans across the E/O transition and through the Miocene (Fig. 2B). The abrupt mid-

Miocene emplacement of the Columbia River Flood Basalt province (34) would also boost silicate weathering, and an uptick in this parameter is noted by Li and Elderfield (20).

Although time-calibrated molecular phylogenies situate the origin of marine diatoms in the early Jurassic ~ 200 Ma (35), it was not until the mid-Cenozoic that this group of marine microalgae rose to ecological and biogeochemical prominence, suggesting that factors other than accelerated silicate weathering were important (13, 36). Unlike other phytoplankton, diatoms are equipped with large intracellular vacuoles (about 40% of the volume of the cell), which they use for the storage of inorganic nutrients. Despite its simplicity, the presence of this organelle provides diatoms superior competitive abilities in turbulent environments where nutrients episodically enter the euphotic zone (37, 38). These environmental conditions became a dominant feature of the Cenozoic oceans in the late Eocene when the spin-up of the circum-Antarctic current and the growth of Antarctic ice sheets amplified the equator to pole heat gradient, and thereby intensified wind-driven ocean upwelling and nutrient supply dynamics (39, 40). The second major pulse of diatom diversification began in the middle Miocene, coinciding with the expansion of Antarctic ice sheets (41) and the global rise of vast grassland ecosystems (42). Grasses contain up to 15% dry weight of silica (43), which forms micromineral deposits (phytoliths) in the cell walls. The expansion of grasses intensified biologically catalyzed weathering processes, accelerating the mobilization of silicate minerals into rivers and ground waters.

Our analysis does not preclude a role for competitive interactions between siliceous plankton to explain the rise of marine diatoms during the Cenozoic era. In steady state, the oceans' carrying capacity for siliceous organisms is controlled by the concentration of H_4SiO_4 in the input flux. Interspecific competition adjusts the abundance of each species according to their specific abilities to take up and use resources. It has been suggested that radiolarians decreased the weight of their silica test as an evolutionary response to increased diatom abundance and H_4SiO_4 limitation (7–9). Our simulations show that a 50% decrease in the silica quota of radiolarians, from an initial Si:C ratio of 106:106 to a value of 53:106 (mol:mol), accounts for ~ 1.4 -fold increase in diatom biomass across the E/O transition (Fig. 3). These results rely on the prescribed decay function that defines the extent to which the silica quota of radiolarians decreased through time. A larger decay predicts an increased effect of siliceous plankton competitive interactions on the ecological success of diatoms (Fig. S5), yet it might violate the premise that radiolarians have a lower silica threshold needed to maintain the functional integrity of their tests.

The observed macroevolutionary decrease in test weight of radiolarians could also be interpreted as an adaptive response to intensifying surface–ocean stratification, which decreased H_4SiO_4 availability in low latitudes (8). Furthermore, with the exception of some species in association with symbiotic algae, radiolarians can reside in deep ocean layers, reducing, to some extent, the significance of competitive interactions between diatoms and radiolarians. Increased ocean stratification and the occurrence of radiolarian populations in deep ocean habitats potentially would have decreased the rate of H_4SiO_4 supply to the euphotic ocean zone, reinforcing the hypothesis that increased continental weathering flux to the ocean was critical to the subsequent rise of diatoms to ecological prominence.

Model simulations and proxy-based calculations of continental silicate weathering fluxes to the oceans suggest an 80% increase in the global biomass of marine diatoms over the last 40 My (Fig. 3). In the contemporary ocean, diatoms dominate the export flux of photosynthetic organic carbon to the ocean interior (44), and thus their emergence and rise to ecological prominence constitutes a relevant landmark in the history of Earth systems that increased the strength and efficiency of the biological pump over

geological time scales. A more efficient biological pump potentially contributed to reduce atmospheric carbon dioxide levels through two different mechanisms, (i) increasing the size of the sedimentary organic carbon reservoir (44, 45) and (ii) promoting the acidic dissolution of deep sea sedimentary carbonates, which increases the oceans' storage capacity for atmospheric carbon dioxide (46, 47). Moreover, diatoms form the basis of some of the most productive food webs in marine ecosystems, and thus their ecological expansion profoundly influenced the flux of energy through these aquatic ecosystems (40, 48). The strong linkage between the erosion of continental silicates and the ecological success of diatoms reported here deserves further investigation, as it might be critical in understanding the long-term dynamics of atmospheric carbon dioxide levels during the Cenozoic and the development of modern marine food webs.

Materials and Methods

We constructed a competition model in which diatoms and radiolarians compete for orthosilicic acid (H_4SiO_4). The model is based on classical competition theory, with two species competing in steady state for a single limiting nutrient. See *SI Text* and *Table S2* for further details. The model incorporates two potential scenarios: (i) a decrease in the weight of radiolarian tests, which is simulated by decreasing the silica to carbon (Si:C) ratio through time, and (ii) an increase in the concentration of H_4SiO_4 in seawater through time. The system is mass conservative such that the total silica concentration in the system remains constant and equal to the initial silica concentration on each time bin. We decrease the Si:C ratio of radiolarians according to an exponential decay function from initial 106:106, 80:106, 53:106, 30:106, and 16:106 ratios on a molar basis. Additionally, we simulated increased H_4SiO_4 input fluxes to the ocean by increasing the steady-state concentration of H_4SiO_4 in the model. The results of the model simulations were compared with estimates of diatom diversity and geographic expansion obtained from global compilations of fossil data.

We calculated changes in the flux of H_4SiO_4 to the oceans over the Cenozoic using the lithium isotope record of seawater ($\delta^7\text{Li}$), a proxy of silicate rock weathering style (16) (Fig. S4). Lithium is a trace element in silicate rocks, and continental weathering accounts for about 1/3 of the lithium flux to the modern ocean basins (the other sources being relatively steady-state

hydrothermal vent and subduction zone reflux; see ref. 16 for a review). There are two stable isotopes of lithium, ^6Li and ^7Li . During chemical weathering of silicates, ^6Li is strongly partitioned into secondary aluminosilicate clays, leaving river waters enriched in ^7Li . The degree of partitioning is a function of the relative completeness of the hydrolysis reactions by which continental silicates are degraded. If the weathering regime is weathering limited (incongruent weathering of, e.g., recently uplifted mountains), the $\delta^7\text{Li}$ value of river waters is expected to be highly fractionated from the host rock, with proportionally more lithium sequestered in secondary clays. Conversely, if the regime is transport limited (more complete weathering), $\delta^7\text{Li}$ will approach the value of the source silicates with relatively more lithium transported in the dissolved fraction.

Using the lithium isotope record of weathering style (variability between dominance by transport-limited and weathering-limited regimes) (16), we calculated the flux of suspended silica to the ocean basins by assuming that the global average ratio of suspended (clay) to dissolved silica in modern rivers is 4:1, while, at ~60 Ma, it was 1:4. This change in ratio is derived from a global lithium mass balance [by Misra and Froelich (16)] that accounts for the fluxes to and from the ocean basins, and reflects the increasingly incomplete weathering of continental silicates driving a significant increase in particulate fraction over the last ~60 My. Li and Elderfield (20) calculate an approximately twofold increase in dissolved silica flux over the same time period, and Misra and Froelich note a ca. 300% increase in total weathered lithium flux from the Paleogene to the present. Hence, we impose a twofold linear increase in H_4SiO_4 content of riverine input over the last 50 My (20), calculate the flux of suspended silica to the ocean basins, and modify our H_4SiO_4 flux accordingly (see Fig. S6 and Dataset S1).

Additionally, the mineral composition of clays in sediments from the Southern Ocean was used as a geographically localized proxy of continental erosion. Illite and chlorite tend to dominate clay assemblages in sediments near regions characterized by weathering-limited regimes where high erosion rates leave fresh rock surfaces continuously exposed to chemical weathering. These data were used to compute relative changes in dissolved silica flux to the oceans as described above.

ACKNOWLEDGMENTS. We thank three anonymous reviewers for helpful comments on the manuscript. P.C. and S.M.V. are supported by Ramon y Cajal contracts from the Spanish Government. This work was supported by Grants 10PXIB312058-PR from Xunta de Galicia and CTM2011-25035 from the Spanish Ministry of Economy and Competitiveness.

1. Egge J, Aksnes D (1992) Silicate as regulating nutrient in phytoplankton competition. *Mar Ecol Prog Ser* 83:281–289.
2. Armbrust EV (2009) The life of diatoms in the world's oceans. *Nature* 459(7244):185–192.
3. Maliva RG, Knoll AH, Siever R (1989) Secular change in chert distribution: A reflection of evolving biological participation in the silica cycle. *Palaios* 4(6):519–532.
4. Siever R (1993) Silica in the oceans: Biological-geochemical interplay. *Scientists on Gaia*, eds Schneider SH, Boston PJ (MIT Press, Cambridge, MA).
5. Finkel ZV, Kotrc B (2010) Silica use through time: Macroevolutionary Change in the morphology of the diatom fustule. *Geomicrobiol J* 27(6-7):596–608.
6. Maldonado M, Carmona MC, Uriz MJ, Cruzado A (1999) Decline in Mesozoic reef-building sponges explained by silicon limitation. *Nature* 401:785–788.
7. Harper HE, Knoll AH (1975) Silica, diatoms, and Cenozoic radiolarian evolution. *Geology* 3(4):175–177.
8. Lazarus DB, Kotrc B, Wulf G, Schmidt DN (2009) Radiolarians decreased silicification as an evolutionary response to reduced Cenozoic ocean silica availability. *Proc Natl Acad Sci USA* 106(23):9333–9338.
9. Moore TC (1969) Radiolaria: Change in skeletal weight and resistance to solution. *Geol Soc Am Bull* 80(10):2103–2108.
10. Falkowski PG, et al. (2004) The evolution of modern eukaryotic phytoplankton. *Science* 305(5682):354–360.
11. Falkowski PG, Schofield O, Katz ME, Schootbrugge B, Knoll AH (2004) Why is the land green and the ocean red? *Coccolithophores*, eds Thierstein H, Young J (Springer, Berlin), pp 429–453.
12. Hannisdal B, Henderiks J, Liow LH (2012) Long-term evolutionary and ecological responses of calcifying phytoplankton to changes in atmospheric CO_2 . *Global Change Biol* 18(12):3504–3516.
13. Lazarus D, Barron J, Renaudie J, Diver P, Türke A (2014) Cenozoic planktonic marine diatom diversity and correlation to climate change. *PLoS ONE* 9(1):e84857.
14. Rabosky DL, Sorhannus U (2009) Diversity dynamics of marine planktonic diatoms across the Cenozoic. *Nature* 457(7226):183–186.
15. Katz ME, Finkel ZV, Grzebyk D, Knoll AH, Falkowski PG (2004) Evolutionary trajectories and biogeochemical impacts of marine eukaryotic phytoplankton. *Annu Rev Ecol Syst* 35(1):523–556.
16. Misra S, Froelich PN (2012) Lithium isotope history of Cenozoic seawater: Changes in silicate weathering and reverse weathering. *Science* 335(6070):818–823.
17. Holland HD (1984) *The Chemical Evolution of the Atmosphere and Oceans* (Princeton Univ Press, Princeton).
18. Froelich F, Misra S (2014) Was the late Paleocene-early Eocene hot because Earth was flat? An ocean lithium isotope view of mountain building, continental weathering, carbon dioxide, and Earth's Cenozoic climate. *Oceanography* 27(1):36–49.
19. Richter FM, Rowley DB, DePaolo DJ (1992) Sr isotope evolution of seawater: The role of tectonics. *Earth Planet Sci Lett* 109(1-2):11–23.
20. Li G, Elderfield H (2013) Evolution of carbon cycle over the past 100 million years. *Geochim Cosmochim Acta* 103:11–25.
21. Moore TC, Jarrard RD, Olivarez Lyle A, Lyle M (2008) Eocene biogenic silica accumulation rates at the Pacific equatorial divergence zone. *Paleoceanography* 23(2):PA2202.
22. Salamy KA, Zachos JC (1999) Latest Eocene–Early Oligocene climate change and Southern Ocean fertility: Inferences from sediment accumulation and stable isotope data. *Palaeogeogr Palaeoclimatol Palaeoecol* 145(1-3):61–77.
23. Tréguer PJ, De La Rocha CL (2013) The world ocean silica cycle. *Annu Rev Mar Sci* 5(1):477–501.
24. Katz ME, et al. (2011) Impact of Antarctic Circumpolar Current development on late Paleogene ocean structure. *Science* 332(6033):1076–1079.
25. Sarmiento JL, Gruber N, Brzezinski MA, Dunne JP (2004) High-latitude controls of thermocline nutrients and low latitude biological productivity. *Nature* 427(6969):56–60.
26. Dürr HH, Meybeck M, Hartmann J, Laruelle GG, Roubeix V (2011) Global spatial distribution of natural riverine silica inputs to the coastal zone. *Biogeochemistry* 8(3):597–620.
27. Viers J, Dupré B, Gaillardet J (2009) Chemical composition of suspended sediments in World Rivers: New insights from a new database. *Sci Total Environ* 407(2):853–868.
28. Chamley H (1990) *Sedimentology* (Springer, New York).
29. Gaillardet J, Dupré B, Louvat P, Allègre CJ (1999) Global silicate weathering and CO_2 consumption rates deduced from the chemistry of large rivers. *Chem Geol* 159(1-4):3–30.
30. Millot R, Gaillardet J, Dupré B, Allègre CJ (2002) The global control of silicate weathering rates and the coupling with physical erosion: New insights from rivers of the Canadian Shield. *Earth Planet Sci Lett* 196(1-2):83–98.
31. Raymo ME, Ruddiman WF (1992) Tectonic forcing of late Cenozoic climate. *Nature* 359(6391):117–122.
32. Kent DV, Muttoni G (2008) Equatorial convergence of India and early Cenozoic climate trends. *Proc Natl Acad Sci USA* 105(42):16065–16070.
33. Goddés Y, et al. (2008) Causal or casual link between the rise of nannoplankton calcification and a tectonically-driven massive decrease in Late Triassic atmospheric CO_2 ? *Earth Planet Sci Lett* 267(1-2):247–255.

34. Barry TL, et al. (2010) New $^{40}\text{Ar}/^{39}\text{Ar}$ dating of the Grande Ronde lavas, Columbia River Basalts, USA: Implications for duration of flood basalt eruption episodes. *Lithos* 118(3-4):213–222.
35. Kooistra WHCF, Gersonde R, Medlin LK, Mann DG (2007) The origin and evolution of the diatoms: Their adaptation to a planktonic existence. *Evolution of Planktonic Photoautotrophs*, eds Falkowski PG, Knoll AH (Academic, Burlington, MA), pp 207–249.
36. Falkowski PG, Oliver MJ (2007) Mix and match: How climate selects phytoplankton. *Nat Rev Microbiol* 5(10):813–819.
37. Cermeño P, Lee J, Wyman K, Schofield O, Falkowski P (2011) Competitive dynamics in two species of marine phytoplankton under non-equilibrium conditions. *Mar Ecol Prog Ser* 429:19–28.
38. Margalef R (1978) Life-forms of phytoplankton as survival alternatives in an unstable environment. *Oceanol Acta* 1(4):493–509.
39. Barker PF, Filippelli GM, Florindo F, Martin EE, Scher HD (2007) Onset and role of the Antarctic Circumpolar Current. *Deep Sea Res Part II* 54(21-22):2388–2398.
40. Berger WH (2007) Cenozoic cooling, Antarctic nutrient pump, and the evolution of whales. *Deep Sea Res Part II* 54(21-22):2399–2421.
41. Flower BP, Kennett JP (1993) Middle Miocene ocean-climate transition: High-resolution oxygen and carbon isotopic records from Deep Sea Drilling Project Site 588A, southwest Pacific. *Paleoceanography* 8(6):811–843.
42. Strömberg CAE (2011) Evolution of grasses and grassland ecosystems. *Annu Rev Earth Planet Sci* 39(1):517–544.
43. Conley DJ (2002) Terrestrial ecosystems and the global biogeochemical silica cycle. *Global Biogeochem Cycles* 16(4):1121.
44. Falkowski P, Laws E, Barber R, Murray J (2003) Phytoplankton and their role in primary, new, and export production. *Ocean Biogeochemistry, Global Change – The IGBP Series*, ed Fasham MR (Springer, Berlin), pp 99–121.
45. Berner RA (2003) The long-term carbon cycle, fossil fuels and atmospheric composition. *Nature* 426(6964):323–326.
46. Archer D, Maier-Reimer E (1994) Effect of deep-sea sedimentary calcite preservation on atmospheric CO_2 concentration. *Nature* 367(6460):260–263.
47. Pälike H, et al. (2012) A Cenozoic record of the equatorial Pacific carbonate compensation depth. *Nature* 488(7413):609–614.
48. Finkel ZV (2007) Does phytoplankton cell size matter? The evolution of modern marine food webs. *Evolution of Primary Producers in the Sea*, eds Falkowski PG, Knoll AH (Elsevier, Boston), pp 333–350.